Inorganic Chemistry

Article

pubs.acs.org/IC

Formation Pathway of Roussin's Red Ester (RRE) via the Reaction of a $\{Fe(NO)_2\}^{10}$ Dinitrosyliron Complex (DNIC) and Thiol: Facile Synthetic Route for Synthesizing Cysteine-Containing DNIC

Chung-Yen Lu and Wen-Feng Liaw*

Department of Chemistry and Frontier Research Center on Fundamental and Applied Sciences of Matters, National Tsing Hua University, Hsinchu 30013, Taiwan

Supporting Information

ABSTRACT: Transformation of $\{Fe(NO)_2\}^{10}$ dinitrosyliron complex (DNIC) $Fe(CO)_2(NO)_2$ into $[\{Fe(NO)_2\}^9]_2$ Roussin's red ester (RRE) $[(\mu\text{-}S(CH_2)_2NH_2)Fe(NO)_2]_2$ (**3**) triggered by cysteamine via the reaction pathway (intermediates) $[\{Fe(NO)_2\}^{10}]_2[(NO)_2Fe(\mu\text{-}CO)(\mu\text{-}S(CH_2)_2NH_3)Fe(NO)_2]$ (**1**) → $\{Fe(NO)_2\}^9\{Fe(NO)_2\}^{10}[(NO)_2Fe(\mu\text{-}S(CH_2)_2NH_2)(\mu\text{-}S(CH_2)_2NH_3)Fe(NO)_2]$ (**2**) → RRE **3** is demonstrated. The **1**-to-**2**-to-**3** conversion is promoted by proton transfer followed by O_2 oxidation and deprotonation. Additionally, a study on facile conversion of complex **3** to complexes $[(SR)(S(CH_2)_2NH_3)Fe(NO)_2]$ [SR = 2-aminoethanethiolate (**4**), benzenethiolate (**5**)] and $[(CysS))(S(CH_2)_2NH_3)Fe(NO)_2]$ (**6**) via reaction with thiols and the further utility of complex **5** as a template for synthesizing mixed-thiolate-containing reduced RRE (rRRE) $[(\mu\text{-}SC_6H_5)(\mu\text{-}S(CH_2)_2NH_3)Fe_2(NO)_4]$ (**7**) provide the methodology for the synthesis and isolation of neutral, pure cysteine-/mixed-thiolate-containing DNIC/RRE. Compared to the conversion of complex **2** to complex **3** via reaction with O_2, diphenyl disulfide triggers oxidation of complex **2** to lead to formation of the neutral $\{Fe(NO)_2\}^9$ DNIC **5** and RRE **3**. S−S bond activation of diphenyl disulfide by rRRE **2** may support the decay (oxidation) of rRRE species in ToMOC via the reduction of adjacent protein residues such as cystins, proposed by Lippard.

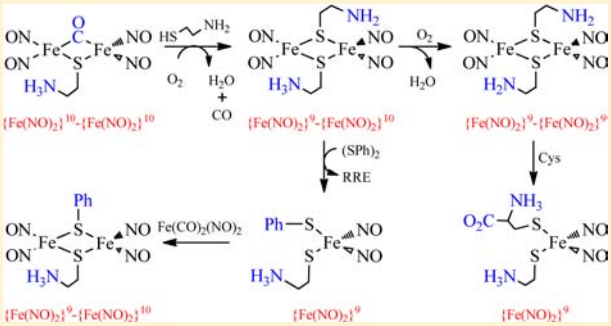

INTRODUCTION

Nitric oxide (NO), known as one of the most versatile species in the biological system, functions as an intracellular second messenger and regulates multiple physiological functions such as vasodilation, neuronal transmission, immune response, and cancer treatment.[1,2] Nitrosylation of [Fe−S] cluster-containing proteins or enzymes in mitochondria producing dinitrosyliron complexes (DNICs) and Roussin's red esters (RREs) has been demonstrated.[3] DNIC has been regarded as one of two possible forms to store and transport NO in biological systems.[4] Protein-bound DNICs, the major species to store and stabilize NO, can be produced by nitrosylation of the chelatable iron pool.[5] In contrast to protein-bound DNICs, low-molecular-weight DNICs (LMW-DNICs) may function as NO-transport and NO-release species in biological systems.[6] Both protein-bound and LMW $\{Fe(NO)_2\}^9$ DNICs display the characteristic electron paramagnetic resonance (EPR) signals at an average g value of 2.03,[1−6,7a−c] while the biomimetic syntheses of six-/five-coordinate $\{Fe(NO)_2\}^9$ DNICs displaying EPR signals g = 2.015−2.02 were reported recently.[7d]

RREs, EPR-silent dinuclear DNICs resulting from antiferromagnetic coupling between two $\{Fe(NO)_2\}^9$ motifs, have been demonstrated to be the major product observed in nitrosylation of the ToMOC Rieske center (toluene/*o*-xylene monooxygenase component C from *Pseudomonas* sp. OX1) and the [4Fe-4S] cluster of Wbl proteins.[8] Further reduction of nitrosylated ToMOC ($ToMOC_{NO}$) with $Na_2S_2O_4$ resulted in the formation of reduced RRE (rRRE) based on the distinctive EPR signals at g = 2.006 and 1.97. Subsequent oxidation of rRRE is ascribed to the reduction of adjacent cystin, as proposed by Lippard.[8a] In chemistry, DNICs and RREs are chemically interconvertible via protonation of DNIC and bridged-thiolate cleavage of RRE, respectively.[9] Three synthetic pathways were explored to produce thiolate-containing $[\{Fe(NO)_2\}^9]_2$ RREs: (i) oxidation (protonation) of the thiolate-containing DNICs; (ii) reaction of $\{Fe(NO)_2\}^{10}$ DNIC $Fe(CO)_2(NO)_2$ with thiols; (iii) alkylation of Roussin's red salt with alkyl halide.[9] We are aware that the water-soluble cysteamine-containing diprotonated RRE $[S((CH_2)_2NH_3)_2Fe_2(NO)_4]SO_4{\cdot}2.5H_2O$ obtained from the addition of a cysteamine hydrochloride aqueous solution into $Fe(SO_4){\cdot}7H_2O$ (molar ratio 1:1) under NO was reported.[10] Actually, synthesis of amino acid containing DNICs and RREs is a challenge because of the unidentified iron nitrosyl products and the unstable nature of amino acid containing DNICs in the presence of O_2 in H_2O, although the cysteine-containing DNICs synthesized from the addition of an aqueous solution of

Received: June 4, 2013
Published: November 22, 2013

L-cysteine into iron salt (molar ratio 20:1) in the presence of NO gas were proposed.[11]

The objectives of this study were (a) to uncover the formation pathway [intermediate(s)] of the neutral $\{Fe(NO)_2\}^9\{Fe(NO)_2\}^9$ RRE deriving from the reaction of cysteamine and $\{Fe(NO)_2\}^{10}$ DNIC $Fe(CO)_2(NO)_2$, (b) to develop a synthetic route for the synthesis and isolation of a pure cysteine-coordinated $\{Fe(NO)_2\}^9$ DNIC,[11] and (c) to explore the methodology of synthesizing the neutral/water-soluble DNIC/RRE containing a biocompatible cysteamine-coordinate ligand as well as the neutral mixed-thiolate-containing DNIC/RRE, which may be crucial to biomedical applications as NO donor species. Specifically, transformation of the neutral $[\{Fe(NO)_2\}^{10}]_2[(NO)_2Fe(\mu\text{-}CO)(\mu\text{-}S(CH_2)_2NH_3)Fe(NO)_2]$ (**1**) → $\{Fe(NO)_2\}^9\{Fe(NO)_2\}^{10}[(NO)_2Fe(\mu\text{-}S(CH_2)_2NH_2)(\mu\text{-}S(CH_2)_2NH_3)Fe(NO)_2]$ (**2**) → $[\{Fe(NO)_2\}^9]_2$ RRE $[(\mu\text{-}S(CH_2)_2NH_2)Fe(NO)_2]_2$ (**3**) was unraveled. The synthetic routes to the neutral $\{Fe(NO)_2\}^9$ DNICs $[(SR)(S(CH_2)_2NH_3)Fe(NO)_2]$ [SR = 2-aminoethanethiolate (**4**) and benzenethiolate (**5**)], $[(Cys)(S(CH_2)_2NH_3)Fe(NO)_2]$ (**6**) containing cysteine-coordinate ligand, and mixed-thiolate-containing rRRE $[(NO)_2Fe(\mu\text{-}SC_6H_5)(\mu\text{-}S(CH_2)_2NH_3)Fe(NO)_2]$ (**7**) were delineated. Of importance, the reaction of rRRE **2** and diphenyl disulfide, yielding $\{Fe(NO)_2\}^9$ DNIC $[(SC_6H_5)(S(CH_2)_2NH_3)Fe(NO)_2]$ (**5**) and RRE **3**, may support the decay (oxidation) of the rRRE in ToMOC via the reduction of adjacent protein residues such as cystins.[8a]

RESULTS AND DISCUSSION

Conversion of the Neutral $[\{Fe(NO)_2\}^{10}]_2$ Mixed-CO-Thiolate-Bridged 1 to rRRE 2 and Then to $[\{Fe(NO)_2\}^9]_2$ RRE 3 Triggered by Cysteamine and O_2. In previous studies,[12] the reaction of $\{Fe(NO)_2\}^{10}Fe(CO)_2(NO)_2$ and thiophenol was presumed to be oxidation/reduction to yield RRE $[(PhS)Fe(NO)_2]_2$ and H_2. Attempts to observe intermediate(s) were not successful; the sole product observed was $[(PhS)Fe(NO)_2]_2$ even at −78 °C. In this study, as shown in Scheme 1a, the reaction of $Fe(CO)_2(NO)_2$ and cysteamine in a 2:1 molar ratio in tetrahydrofuran (THF) at 0 °C yielded the thermally stable, neutral $[\{Fe(NO)_2\}^{10}]_2$ dinuclear DNIC **1** (yield 78%) bearing bridging CO and $[S(CH_2)_2NH_3]$ ligands. Complex **1** was characterized by IR, UV−vis, ^1H NMR [Supporting Information (SI) Figure S1], and single-crystal X-ray diffraction (XRD). It is noticed that the formation of anionic $[(NO)_2Fe(\mu\text{-}CO)(\mu\text{-}SC_6H_4\text{-}o\text{-}N(CH_3)_2)Fe(NO)_2]^-$ (**1-Ph**), displaying IR ν_{NO}/ν_{CO} stretching frequencies at 1691 s, 1705 s (ν_{NO}), and 1843 m (ν_{CO}) cm^{-1} (THF), via coordination of $\{Fe(NO)_2\}^{10}[(TMEDA)Fe(NO)_2]$ to $\{Fe(NO)_2\}^{10}[(SC_6H_4\text{-}o\text{-}N(CH_3)_2)Fe(NO)_2]^-$ was reported.[13a] Despite the presumed stronger electron-donating ability of $[^-SC_2H_4NH_3^+]$, compared to $[SC_6H_4\text{-}o\text{-}N(CH_3)_2]^-$, the NH···S hydrogen-bonding interaction within the bridging thiolate ligand of complex **1** rationalizes the IR ν_{NO}/ν_{CO} stretching frequencies at 1693 s, 1707 s (ν_{NO}), and 1851 m (ν_{CO}) cm^{-1} (THF) exhibited by complex **1**.[13b] Ligand-substitution coupled proton transfer rationalizes the formation of complex **1** upon reaction of $Fe(CO)_2(NO)_2$ with cysteamine in a 2:1 molar ratio. The magnetic measurement of complex **1** is in accordance with the diamagnetic form. The $[Fe(\mu\text{-}C)(\mu\text{-}S)Fe]$ core geometry of complex **1** is best described as a planar rhombus (Figure 1), in contrast to a butterfly-like structure with a dihedral angle of 170.1° (the intersection of the Fe_2S and Fe_2C

Scheme 1

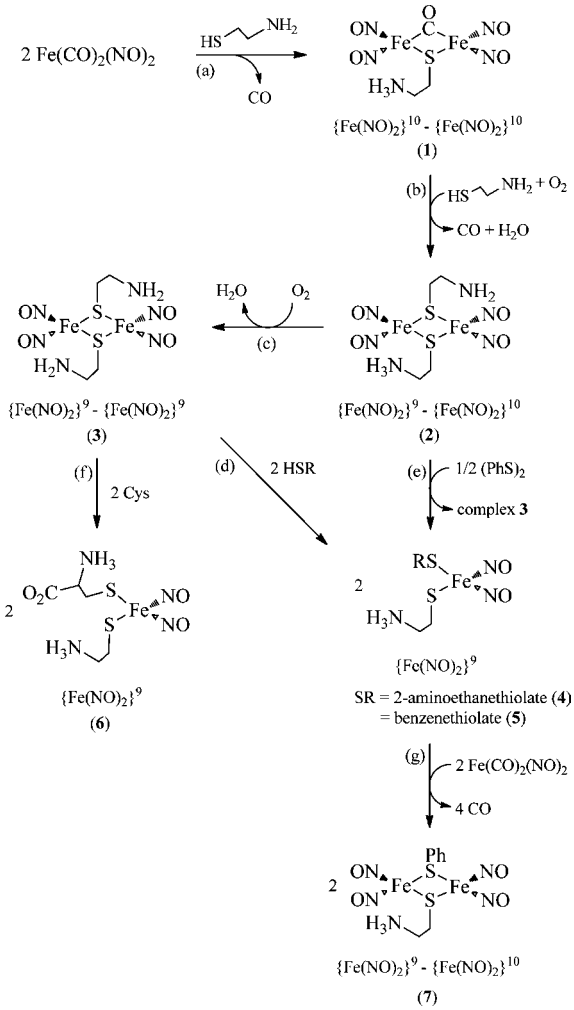

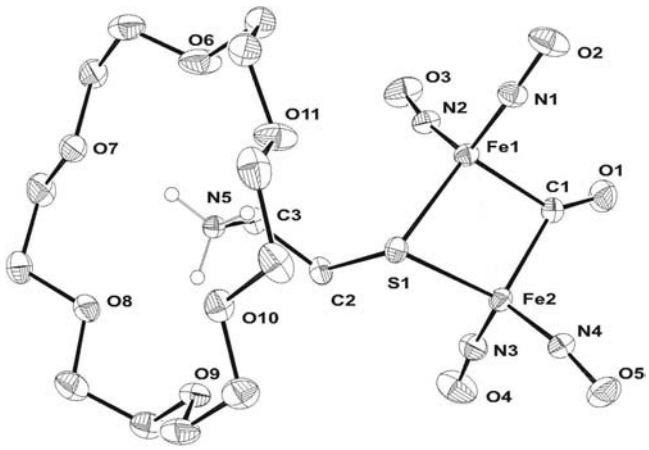

Figure 1. ORTEP drawing and labeling scheme of complex **1** with thermal ellipsoids drawn at 30% probability. Selected bond lengths (Å) and angles (deg): Fe1···Fe2 2.629(1), C1−Fe1 1.991(3), C1−Fe2 1.993(3), Fe1−N1 1.658(3), Fe1−N2 1.646(3), Fe2−N3 1.651(3), Fe2−N4 1.657(3), Fe1−S1 2.284(1), Fe2−S1 2.268(1), C1−O1 1.135(4), N1−O2 1.186(4), N2−O3 1.190(3), N3−O4 1.178(4), N4−O5 1.189(3); Fe1−C1−Fe2 82.6(2), Fe2−S1−Fe1 70.5(1), C1−Fe1−S1 103.1(1), C1−Fe2−S1 103.7(1), N2−Fe1−N1 119.4(2), N3−Fe2−N4 116.0(1), O2−N1−Fe1 169.9(2), O3−N2−Fe1 171.5(3), O4−N3−Fe2 170.9(3), O5−N4−Fe2 168.5(3).

dx.doi.org/10.1021/ic402364p | Inorg. Chem. 2013, 52, 13918−13926

Table 1. Selected Bond Lengths (Å) of the $[\{Fe(NO)_2\}^9]_2$ RRE, $\{Fe(NO)_2\}^9\{Fe(NO)_2\}^{10}$ rRRE, and $[\{Fe(NO)_2\}^{10}]_2$ rRRE[13a,14,15a]

complex	Fe···Fe	Fe−S	Fe−N(O)	N−O
$\{Fe(NO)_2\}^9\{Fe(NO)_2\}^9$				
$[(\mu\text{-}S^tBu)Fe(NO)_2]_2$	2.705(1)	2.253(1)	1.668(1)	1.169(2)
$\{Fe(NO)_2\}^9\{Fe(NO)_2\}^{10}$				
$[(\mu\text{-}S^tBu)Fe(NO)_2]_2^-$	2.958(1)	2.303(1)	1.662(2)	1.186(3)
2	2.887(2)	2.312(2)	1.675(5)	1.177(6)
$\{Fe(NO)_2\}^{10}\{Fe(NO)_2\}^{10}$				
$[(\mu\text{-}S^tBu)Fe(NO)_2]_2^{2-}$	3.437(1)	2.348(1)	1.637(3)	1.223(3)
1	2.630(1)	2.276(1)	1.653(3)	1.186(4)
1-Ph[a]	2.591(1)	2.278(1)	1.659(2)	1.180(3)

[a]Complex **1-Ph** stands for $[(NO)_2Fe(\mu\text{-}CO)(\mu\text{-}SC_6H_4\text{-}o\text{-}N(CH_3)_2)Fe(NO)_2]^-$.[13a]

planes) observed in the $[\{Fe(NO)_2\}^{10}]_2$ **1-Ph**.[13a] On the basis of the Fe−N(O) and N−O bond lengths, the average Fe−N(O) and N−O bond lengths of 1.653(3) and 1.186(4) Å, respectively, for complex **1** also support a $[\{Fe(NO)_2\}^{10}]_2$ electronic structure of the $\{Fe(NO)_2\}\{Fe(NO)_2\}$ core of dimeric DNIC **1** {1.650(7)−1.638(3) Å [Fe−N(O)] and 1.214(6)−1.189(4) Å (N−O) for $\{Fe(NO)_2\}^{10}$ DNICs}.[14] Compared to the Fe···Fe distance of 3.437(1) Å found in $[\{Fe(NO)_2\}^{10}]_2$ drRRE $[(\mu\text{-}S^tBu)Fe(NO)_2]_2^{2-}$,[14a] the apparently shorter Fe(1)···Fe(2) distances of 2.630(1) Å observed in complex **1** and 2.591(1) Å observed in complex **1-Ph** indicate a greater extent of Fe1···Fe2 bonding interaction in complex **1** (Table 1).[13a] The interpretation here is that CO bridges two iron atoms, increasing Fe → CO π-back-bonding with a concomitant gain in the Fe···Fe bonding interaction and reimbursing the deficiency of the electron density surrounding the iron cores. Specifically, the shortening of the Fe···Fe distance [2.630(1) Å] of complex **1**, compared to that of $[(\mu\text{-}S^tBu)Fe(NO)_2]_2^{2-}$,[14] is employed to reimburse the electronic deficiency induced by Fe → CO π-back-bonding to stabilize complex **1**.[13a] The generally shorter Fe−C(O) bond, however, also leads to contraction of the Fe···Fe distance. The average Fe−N(O) and N−O bond lengths for various dinuclear DNICs in Table 1 reflect expected changes as the π-accepting abilities of the bridging ligands (CO > $[S(CH_2)_2NH_3]$ > $[S^tBu]^-$) and electronic structures of $\{Fe(NO)_2\}^n\{Fe(NO)_2\}^m$ cores (n = 9, 10; m = 9, 10) are varied. It is noticed that the lengthening in the average N−O bond length from 1.169(2) Å for $[\{Fe(NO)_2\}^9]_2[(\mu\text{-}S^tBu)Fe(NO)_2]_2$ to 1.186(4) Å for $[\{Fe(NO)_2\}^{10}]_2$ complex **1** accompanied by the shortening in the average Fe−N(O) bond distance from 1.668(1) Å ($[(\mu\text{-}S^tBu)Fe(NO)_2]_2$) to 1.653(3) Å (complex **1**) is comparable to the lengthening and shortening of N−O and Fe−N(O) bond lengths, respectively, occurring from reduction of $[\{Fe(NO)_2\}^9]_2[(\mu\text{-}S^tBu)Fe(NO)_2]_2$, yielding $\{Fe(NO)_2\}^9[\{Fe(NO)_2\}^{10}$ rRRE $[(\mu\text{-}S^tBu)Fe(NO)_2]_2^-$ (Table 1).[14,15a]

As shown in Scheme 1b, the lability of the bridging CO of complex **1** was demonstrated by reaction of complex **1** with cysteamine and O_2 in THF. Treatment of the THF solution of complex **1** with cysteamine and O_2 in a 1:1:0.5 molar ratio at ambient temperature led to the shift in IR spectra from 1693 s, 1707 s (ν_{NO}), 1851 s (ν_{CO}) cm^{-1} (THF) to 1658 s, 1678 s (ν_{NO}) cm^{-1}, consistent with the formation of rRRE **2** (SI Figures S2 and S3). With the aid of isotopic labeling experiments, the reaction of a THF solution of complex **1**, D-cysteamine $[DS(CH_2)_2NH_2]$, and O_2 in a 1:1:0.5 molar ratio yields the byproduct DHO identified by ^2H NMR [δ 2.57 ppm (THF); SI Figure S4]. Instead of a $[K^+]$ or $[PPN^+]$ countercation, protonation of the pendant amine group, which is stabilized by coordination to crown ether, affords the first example of the neutral rRRE **2** containing the fully delocalized $\{Fe(NO)_2\}^9\{Fe(NO)_2\}^{10}$ electronic structure.[14b,c] The conversion of complex **1** to complex **2** upon adding 1 equiv of cysteamine and 0.5 equiv of O_2 into complex **1** in THF was also observed by UV−vis spectroscopy at 298 K; the intense bands at 387 and 605 nm disappeared, accompanied by the simultaneous formation of absorption bands 452, 650, and 962 nm. The UV−vis spectrum of complex **2** exhibits an intense obsorption around 962 nm (1380 cm^{-1} M^{-1}), which may be attributed to the intervalence transition of the fully delocalized mixed-valence complexes.[14b,c] At 77 K, complex **2** displays an axial EPR signal at $g_\perp$ = 2.011 and $g_\parallel$ = 1.968 and an isotropic EPR signal at g = 1.998 at 298 K (Figure 2), consistent with the characteristic axial EPR signal ($g_\perp$ = 2.009 and $g_\parallel$ = 1.965 at 77K) of the rRRE $[(\mu\text{-}S^tBu)Fe(NO)_2]_2^-$.[14b,c] The magnetic susceptibility value of the powder sample of complex **2** decreased from 1.83 cm^3 mol^{-1} at 300 K to 1.34 cm^3 mol^{-1} at 4 K. The corresponding temperature-independent μ_{eff} value of 1.75 μ_B suggests that the magnetic ground state is a $S = {}^1/_2$ system resulting from strong antiferromagnetic coupling between the iron atoms and nitroxyl groups. The shorter Fe···Fe distance of 2.887(2) Å in complex **2** (Figure 3), compared to the Fe···Fe distance of 2.958(1) Å in the complex $[(S^tBu)Fe(NO)_2]_2^-$,[14b,c] also supports the fully delocalized $[\{Fe(NO)_2\}^9\{Fe(NO)_2\}^{10}]$ electronic structure of the neutral rRRE **2** (Table 1). Presumably, the electronic perturbation caused by the nitrogen protonation of $[(NO)_2Fe(\mu\text{-}SC_2H_4NH_2)]_2^-$ triggers the stronger Fe1···Fe2 interaction accompanied by lengthening Fe−N(O) and shortening N−O bond lengths, compared to the anionic rRRE $[(S^tBu)Fe(NO)_2]_2^-$ [1.675(5) vs 1.662(2) Å and 1.177(6) vs 1.186(3) Å; Table 1].[14b,c] O_2 oxidation of complex **1** accompanied by deprotonation yielding H_2O and the proposed thermally unstable $\{Fe(NO)_2\}^9\{Fe(NO)_2\}^{10}[(NO)_2Fe(\mu\text{-}S(CH_2)_2NH_2)(\mu\text{-}CO)Fe(NO)_2]$ intermediate and then nucleophilic attack of cysteamine on the iron site followed by CO-ligand displacement may rationalize the conversion of $[\{Fe(NO)_2\}^{10}]_2$ complex **1** to $\{Fe(NO)_2\}^9\{Fe(NO)_2\}^{10}$ complex **2**. The synthetic method described above may act as an accessible alternative reaction pathway to generate neutral thiolate-containing $[\{Fe(NO)_2\}^9\{Fe(NO)_2\}^{10}]$ rRRE, in contrast to reduction of $[\{Fe(NO)_2\}^9]_2$ RRE, yielding the anionic rRRE observed in the previous study.[14b,c]

Upon the addition of dry O_2 into the THF solution of complex **2** (Scheme 1c), a pronounced color change from dark green to red brown occurs at ambient temperature. The higher-

dx.doi.org/10.1021/ic402364p | Inorg. Chem. 2013, 52, 13918−13926

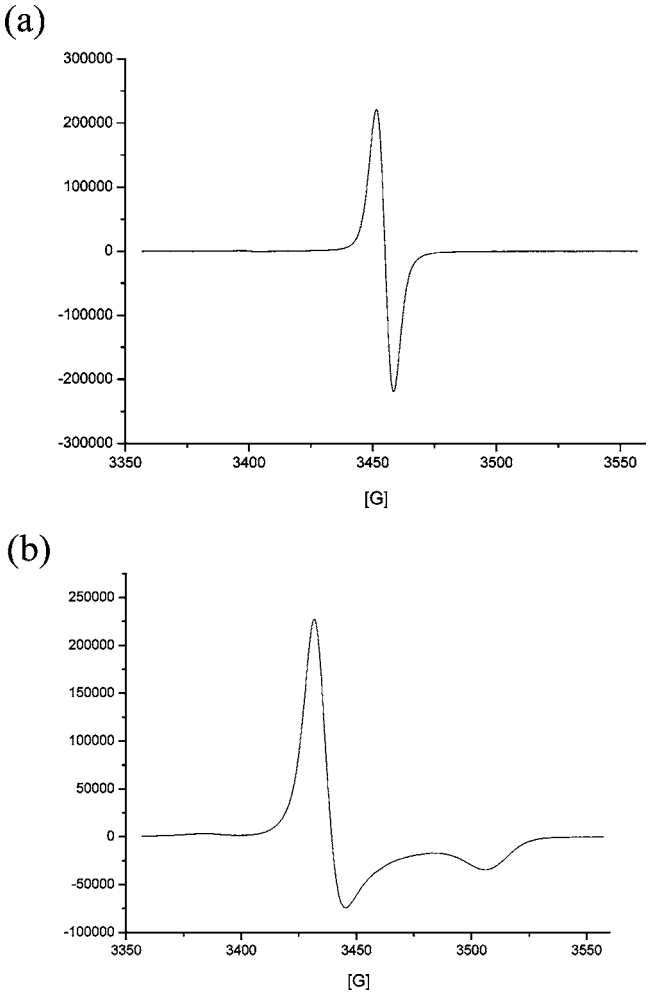

Figure 2. EPR spectra of complex **2** in THF (a) at 298 K (g_{av} = 1.998) and (b) at 77 K ($g_{\perp}$ = 2.011; $g_{\parallel}$ = 1.968).

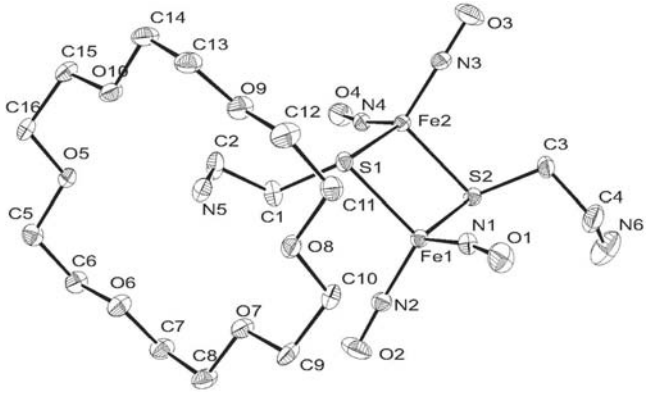

Figure 3. ORTEP drawing and labeling scheme of complex **2** with thermal ellipsoids drawn at 30% probability. Selected bond lengths (Å) and angles (deg): Fe1···Fe2 2.887(2), N1–Fe1 1.676(5), N2–Fe1 1.676(5), N3–Fe2 1.672(5), N4–Fe2 1.675(5), S1–Fe1 2.322(2), S1–Fe2 2.329(2), S2–Fe2 2.298(2), S2–Fe1 2.299(2), N1–O1 1.173(6), N2–O2 1.173(6), N3–O3 1.177(7), N4–O4 1.184(6); N2–Fe1–N1 118.4(2), N3–Fe2–N4 119.6(2), S2–Fe1–S1 102.8(1), S2–Fe2–S1 102.7(1), Fe1–S1–Fe2 76.7(1), Fe2–S2–Fe1 77.8(1), O1–N1–Fe1 169.6(5), O2–N2–Fe1 171.4(5), O3–N3–Fe2 170.5(5), O4–N4–Fe2 169.7(4).

energy ν_{NO} bands [1749 s, 1774 s, 1808 w cm^{-1} (THF)] shifted by $\Delta\nu_{NO}$ = ~93 cm^{-1} from those of complex **2** imply variation in the electronic structure of the $[Fe(NO)_2Fe(NO)_2]$ motif.[15,16] The UV–vis, IR (SI Figure S5), and ^1H NMR (SI Figure S6) studies confirmed the formation of the oily $[\{Fe(NO)_2\}^9]_2$ dinuclear DNIC $[(NO)_2Fe(\mu\text{-}S(CH_2)_2NH_2)]_2$ (**3**) along with byproduct H_2O identified by ^1H NMR.[15]

Synthesis of the Neutral $\{Fe(NO)_2\}^9$ Mixed-Thiolate-Containing DNICs and Reactivity Study of rRRE 2. As observed in the previous study that the steric effect of the nucleophiles ($[EtS]^-$ vs $[^tBuS]^-$) on controlling the reduction and bridged-thiolate cleavage of RREs yielding rRRE $[(\mu\text{-}SR)Fe(NO)_2]_2^-$ and DNIC $[(SR)_2Fe(NO)_2]^-$, respectively,[14c] the direct conversion of complex **3** to the neutral $\{Fe(NO)_2\}^9$ DNIC $[(S(CH_2)_2NH_2)(S(CH_2)_2NH_3)Fe(NO)_2]$ (**4**) was observed when a MeOH solution of complex **3** was treated with 2 equiv of cysteamine at ambient temperature (Scheme 1d). In a similar fashion, the reaction of thiophenol and complex **3** in THF led to formation of the neutral $\{Fe(NO)_2\}^9$ DNIC $[(SC_6H_5)(S(CH_2)_2NH_3)Fe(NO)_2]$ (**5**). Complexes **4** and **5** were characterized by IR (SI Figure S5), UV–vis, EPR, and single-crystal XRD. Presumably, the reaction proceeds via amine protonation of the bridging $[S(CH_2)_2NH_2]$ of complex **3** to yield the proposed intermediate $[(NO)_2Fe(\mu\text{-}S(CH_2)_2\text{-}NH_3)]_2^{2+}$, after which $[S(CH_2)_2NH_2]^-$ (or $[SPh]^-$) binding to the electron-deficient $[\{Fe(NO)_2\}^9]_2$ core of intermediate $[(NO)_2Fe(\mu\text{-}S(CH_2)_2NH_3)]_2^{2+}$ affords complex **4** (or **5**). In comparison with the IR ν_{NO} stretching frequencies at 1672, 1715 cm^{-1} exhibited by complex $[(SEt)_2Fe(NO)_2]^-$, the hydrogen-bonding interaction between the pendant ammonium group and the coordinated 2-aminoethanethiolate in complex **4** shifted the IR ν_{NO} stretching frequencies to 1688 s, 1733 s cm^{-1}.[13,16] Complex **4** is stable in MeOH at ambient temperature and exhibits an isotropic EPR signal g_{av} = 2.029 at 298 K [a rhombic pattern with principal g values of g_1 = 2.039, g_2 = 2.029, and g_3 = 2.014 at 77 K (MeOH)]. Single-crystal X-ray structures of complexes **4** and **5** are depicted in Figures 4 and 5, and selected bond dimensions are presented in

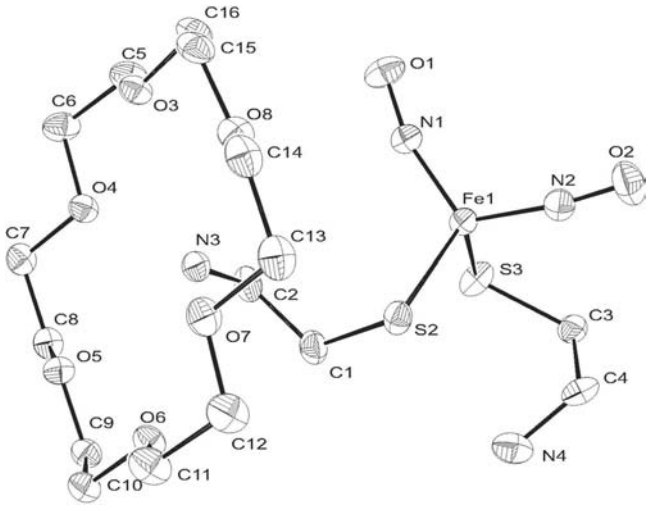

Figure 4. ORTEP drawing and labeling scheme of complex **4** with thermal ellipsoids drawn at 30% probability. Selected bond lengths (Å) and angles (deg): N1–Fe1 1.685(3), N2–Fe1 1.672(3), S2–Fe1 2.293(1), S3–Fe1 2.251(1), N1–O1 1.180(3), N2–O2 1.168(3); N2–Fe1–N1 116.6(1), S3–Fe1–S2 107.7(1), O1–N1–Fe1 163.2(3), O2–N2–Fe1 171.2(2).

dx.doi.org/10.1021/ic402364p | Inorg. Chem. 2013, 52, 13918–13926

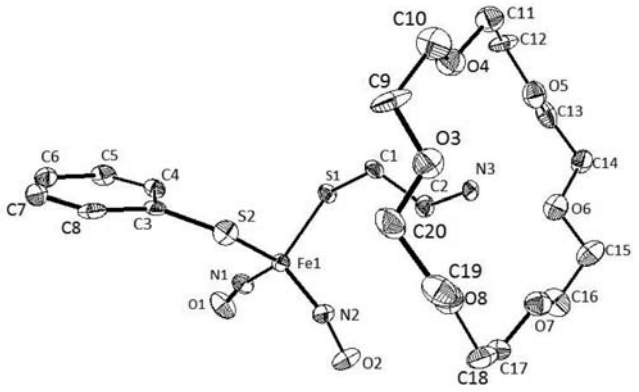

Figure 5. ORTEP drawing and labeling scheme of complex **5** with thermal ellipsoids drawn at 30% probability. Selected bond lengths (Å) and angles (deg): N1−Fe1 1.648(7), N2−Fe1 1.662(6), S1−Fe1 2.280(2), S2−Fe1 2.276(2), N1−O1 1.165(7), N2−O2 1.169(7); N1−Fe1−N2 112.4(3), S2−Fe1−S1 109.8(1), O1−N1−Fe1 168.2(6), O2−N2−Fe1 164.2(6).

the figure caption. Presumably, the electronic perturbation caused by nitrogen protonation of the $[NH_2(CH_2)_2S]$ ligand of complex **4** results in elongation of the Fe1−S2 distance [2.293(1) Å], compared to the Fe1−S3 distance of 2.251(1) Å.

Of importance, when 0.5 equiv of $(SPh)_2$ was added to the THF solution of complex **2** and stirred for 3 h at ambient temperature, a reaction occurred to afford complex **5** accompanied by formation of the well-known complex **3** (Scheme 1e), characterized by IR, UV−vis, and single-crystal XRD.

Synthesis of Cysteine-Containing DNIC and Mixed-Thiolate-Containing rRRE. In spite of the few reported syntheses of cysteine-containing DNIC,[11] synthesis and isolation of pure amino acid containing DNICs is a challenge because of the unidentified iron nitrosyl products and the unstable nature of amino acid containing DNICs in the presence of O_2 in H_2O.[17] The water-soluble complex **3** developed in this study may bear the potential to serve as the starting species to synthesize cysteine-containing DNICs. As shown in Scheme 1f, the addition of 2 equiv of cysteine to a solution of complex **3** in MeOH led to isolation of the olive solid $[(SC_2H_3(CO_2)(NH_3))(S(CH_2)_2NH_3)Fe(NO)_2]$ (**6**; yield 76%) characterized by IR, UV−vis, and EPR. Complex **6** is moderately air-sensitive but thermally stable in solid and aqueous solution at room temperature. The Fourier transform infrared (FTIR) spectrum of complex **6** in aqueous solution (D_2O) is depicted in Figure 6. Compared to the cysteine-containing DNIC $[(Cys)_2Fe(NO)_2]^-$ and peptide KCAACK-bound DNIC $[(KCAACK)Fe(NO)_2]$ displaying IR 1727 s, 1772 s (ν_{NO}) cm^{-1} and 1720 s, 1767 s (ν_{NO}) cm^{-1}, respectively, in H_2O,[17] the aqueous (D_2O) IR ν_{NO} spectrum of complex **6** exhibits the diagnostic stretching frequencies 1719 s, 1770 s (ν_{NO}) cm^{-1} [1710 m, 1751 s (ν_{NO}) cm^{-1} (MeOH)]. We noticed that the UV−vis spectrum (absorption band at 378 nm) of complex **6** in H_2O is almost the same as those of $\{Fe(NO)_2\}^9[(Cys)_2Fe(NO)_2]^-$ [405 nm (H_2O)] and peptide KCAACK-bound DNIC $[(KCAACK)Fe(NO)_2]$ [409 nm (H_2O)] (Figure 7).[17] Complex **6** displays a well-resolved 13-line hyperfine-splitting EPR spectrum g value of 2.03. With the aid of the EPR spectrum of complex $[(C_3H_3N_2)(SC_2H_5)Fe(NO)_2]^-$ showing the hyperfine coupling constants $A_{N(NO)}$ = 2.50 G and $A_{H(-SCH_2)}$ = 1.55 G at 298 K,[17b] the EPR splitting

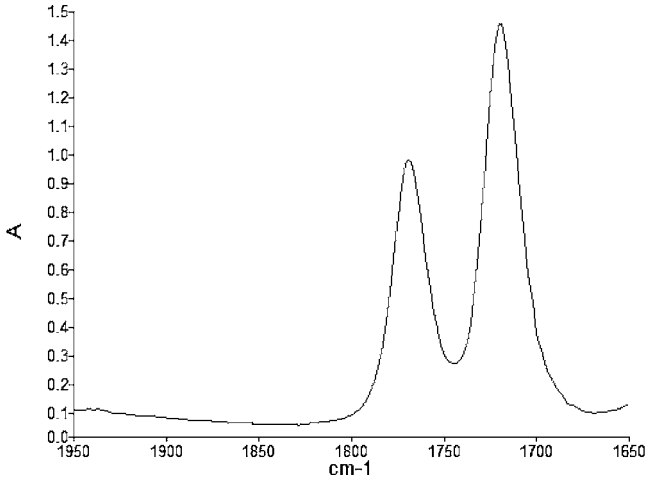

Figure 6. Aqueous IR spectrum [1719 s, 1770 s (ν_{NO}) cm^{-1} (D_2O)] of complex **6**.

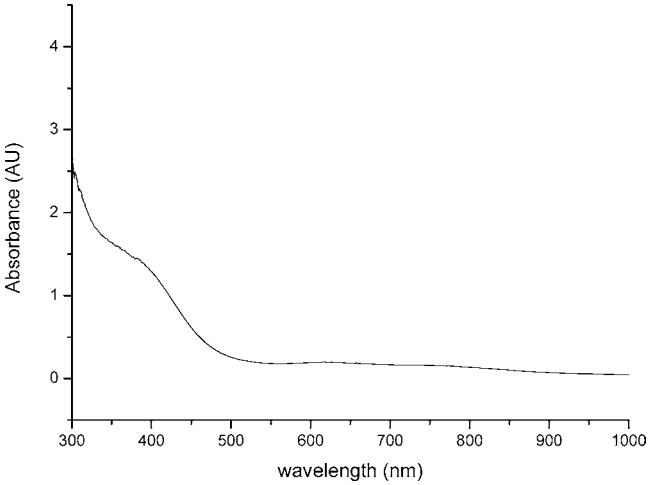

Figure 7. Aqueous UV−vis spectrum of complex **6** with an absorption band at 378 nm.

lines of complex **6** can be rationalized by the unpaired electron coupling with the nitrosyl groups (g = 2.03; $A_{N(NO)}$ = 2.36 G), and hydrogen atoms of cysteine ($A_{H(Cys)}$ = 1.15 G) and cysteamine ($A_{H(cysteamine)}$ = 1.45 G) (H_2O) at 298 K (Figure 8), compared to $[(Cys)_2Fe(NO)_2]^-$ showing a well-resolved 13-line hyperfine-splitting EPR g value of 2.031 with coupling constant $A_{N(NO)}$ = 2.2 G ($A_{H(Cys)}$ = 1.18 G) at 298 K and $[(KCAACK)Fe(NO)_2]$ exhibiting a 7-line EPR spectrum with a g value of 2.029 ($A_{N(NO)}$ = 2.45 G; $A_{H(Cys)}$ = 1.90 G) at 298 K.[17,18] These results imply that this is an efficient pathway (method) to synthesize the pure/isolated cysteine-containing DNIC, in contrast to cysteine-containing DNIC obtained from the addition of NO(g) to an aqueous solution of L-cysteine and iron salt (molar ratio 20:1) and characterized by EPR.[11]

The successful synthesis of complex **5** provides a prospective route for the synthesis of RRE containing asymmetric bridging thiolate ligands. As a consequence, the reaction of complex **5** and $[Fe(CO)_2(NO)_2]$ was investigated. Upon the addition of 1 equiv of $[Fe(CO)_2(NO)_2]$ to a solution of complex **5** in THF at ambient temperature, the IR ν_{NO} stretching frequency shifting from 1739 s, 1693 s (ν_{NO}) cm^{-1} (THF) to 1665 s, 1685 s (ν_{NO}) cm^{-1} implied the formation of the neutral rRRE $[(NO)_2Fe(\mu\text{-}SC_6H_5)(\mu\text{-}S(CH_2)_2NH_3)Fe(NO)_2]$ (**7**), which is

dx.doi.org/10.1021/ic402364p | Inorg. Chem. 2013, 52, 13918−13926

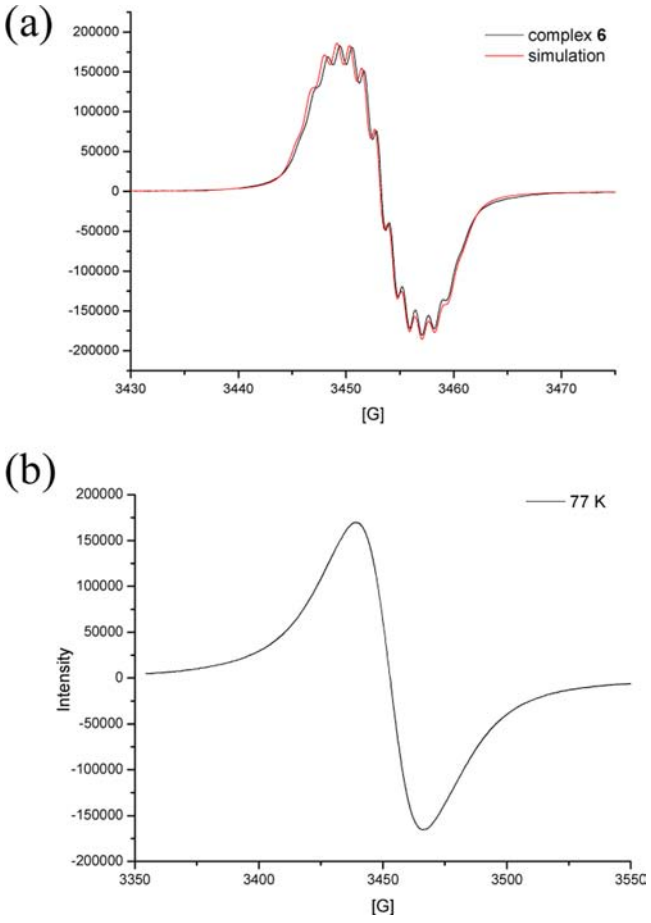

Figure 8. EPR spectra of complex **6** in H_2O (a) at 298 K (g_{av} = 2.03, $A_{N(NO)}$ = 2.36 G, $A_{H(Cys)}$ = 1.15 G, and $A_{H(cysteamine)}$ = 1.45 G) and (b) at 77 K (g_1 = 2.038, g_2 = 2.030, and g_3 = 2.021).

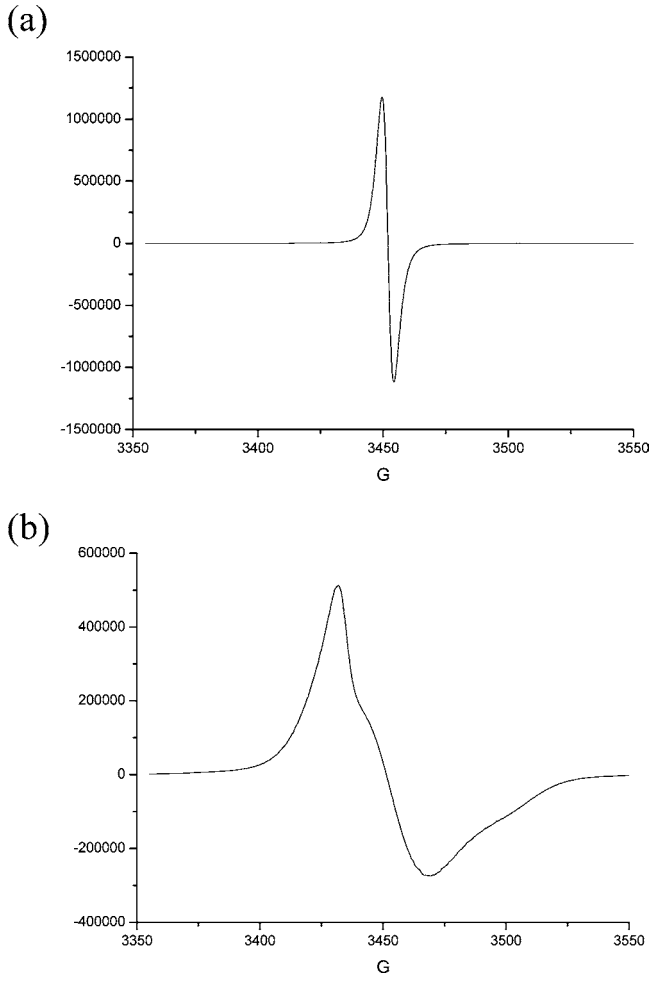

Figure 9. EPR spectra of complex **7** in THF (a) at 298 K (g_{av} = 1.999) and (b) at 77 K (g_1 = 2.010, g_2 = 1.999, and g_3 = 1.972).

the first example of rRRE containing the mixed-bridging thiolates (Scheme 1g).[14b,c] Complex **7** containing the mixed-bridging thiolates exhibits an isotropic EPR signal at g = 1.999 at 298 K and a rhombic EPR signal at g_1 = 2.010, g_2 = 1.999, and g_3 = 1.972 (THF) at 77 K (Figure 9), deviating from the characteristic axial EPR signal ($g_\perp$ = 2.008 and $g_\parallel$ = 1.968 at 77 K) of the rRRE $[(\mu\text{-SEt})Fe(NO)_2]_2^-$.[14b,c] The Fe K-edge pre-edge energy derived from the 1s → 3d transition in a distorted T_d environment of the iron centers is 7113.4 eV for complex **7**, comparable to that (7113.4 eV) of $\{Fe(NO)_2\}^9\{Fe(NO)_2\}^{10}[(NO)_2Fe(\mu\text{-}S^tBu)]_2^-$.[19] Complex **7** displays air sensitivity. When dry O_2 was added to the THF solution of complex **7** at ambient temperature, the reaction led to the formation of $[\{Fe(NO)_2\}^9]_2$ RRE $[(NO)_2Fe(\mu\text{-}SC_6H_5)(\mu\text{-}S(CH_2)_2NH_2)Fe(NO)_2]$ (**8**) characterized by IR [1754 s, 1780 s, 1812 w cm^{-1} (THF)] spectra, instead of the rearrangement products $[(NO)_2Fe(\mu\text{-SPh})]_2$ [IR ν_{NO} 1757 s, 1784 s, 1814 vw cm^{-1} (THF)] and complex **3** [IR ν_{NO} 1749 s, 1774 s, 1808 vw cm^{-1}(THF)].

■ CONCLUSION AND COMMENTS

Studies on the reaction of $\{Fe(NO)_2\}^{10}Fe(CO)_2(NO)_2$ and thiol (cysteamine), yielding RRE **3**, and methodology of synthesizing cysteine-containing DNIC have led to the following results:

(1) This study demonstrates that the reaction of $\{Fe(NO)_2\}^{10}$ DNIC $Fe(CO)_2(NO)_2$ and cysteamine yields RRE **3** via the reaction process (intermediates) **1** → neutral **2** → **3**. The **1**-to-**2**-to-**3** conversion is promoted by proton transfer followed by O_2 oxidation and deprotonation, instead of the oxidative addition of RSH (R = Ph, alkyl) onto $\{Fe(NO)_2\}^{10}$ DNIC $Fe(CO)_2(NO)_2$ followed by reductive elimination of H_2 affording RRE $[(\mu\text{-SR})Fe(NO)_2]_2$.

(2) In spite of EPR-characterized cysteine-containing DNIC obtained from the assembly of cysteine, iron salt, and free NO reported,[10,11] this study shows RRE **3** to be a convenient starting material for synthesis and isolation of the pure amino acid-containing $\{Fe(NO)_2\}^9$ DNIC **6** and the further utility of RRE **3** as $\{Fe(NO)_2\}$ reservoirs for synthesizing mixed-thiolate-containing monomeric DNICs.

(3) The effective CO-π-accepting functionality is responsible for stabilizing the neutral $[\{Fe(NO)_2\}^{10}]_2$ dinuclear DNIC **1**. The addition of cysteamine and 0.5 equiv of O_2 into complex **1** may serve as an accessible alternative synthetic strategy to produce the neutral thiolate-containing $[\{Fe(NO)_2\}^9\{Fe(NO)_2\}^{10}]$ rRRE **2**, in contrast to reduction of $[\{Fe(NO)_2\}^9]_2$ RRE, yielding the anionic rRRE uncovered in the previous study.[14b,c]

(4) The mixed-bridging thiolate-containing rRRE **7**, obtained from the coordinative addition of complex **5** to $[Fe(CO)_2(NO)_2]$, displays a rhombic EPR signal at g_1 = 2.010, g_2 = 1.999, and g_3 = 1.972 (THF) at 77 K, deviated from the characteristic axial EPR signal of the rRRE $[(\mu\text{-SEt})_2Fe$-

dx.doi.org/10.1021/ic402364p | Inorg. Chem. 2013, 52, 13918−13926

$(NO)_2]_2^-$ ($g_\perp$ = 2.008 and $g_\parallel$ = 1.968 at 77 K) and the neutral rRRE **2** ($g_\perp$ = 2.011 and $g_\parallel$ = 1.968 (THF) at 77 K).[14b,c]

Our results bridging the study of the formation pathway of RRE and investigation of the reactivity and spectral characteristics of the newly synthesized DNICs/RREs provide the methodology (prospective) to synthesize the neutral, water-soluble DNICs/RREs containing asymmetric thiolate-coordinated ligands, which may be crucial to biomedical applications as NO donor species. In addition, the neutral rRRE **2**-mediated S−S bond activation of $(PhS)_2$ to produce the neutral $\{Fe(NO)_2\}^9$ DNIC **5** and RRE **3** may lend support to the proposal that the decay (oxidation) of rRRE in ToMOC corresponds to reduction of the disulfide bonds of the adjacent cystins, reported by Lippard.[8a]

EXPERIMENTAL SECTION

Manipulations, reactions, and transfers of samples were conducted under nitrogen according to standard Schlenk techniques or in a glovebox (nitrogen gas). Solvents were distilled under nitrogen from appropriate drying agents (diethyl ether from CaH_2 and hexane and THF from sodium benzophenone) and stored in dried, nitrogen-filled flasks over 4 Å molecular sieves. Nitrogen was purged through these solvents before use. The solvent was transferred to a reaction vessel via a stainless steel cannula under positive pressure of nitrogen. The reagents cysteamine, thiophenol, L-cysteine, 18-crown-6-ether (TCI/Alfa/Aldrich/Eskay Engiechem), and O_2 (San fu, 99.9%) were used as received, and complex $[Fe(CO)_2(NO)_2]$ was synthesized on the basis of the reported literature.[20] IR spectra ν_{NO}/ν_{CO} stretching frequencies were recorded on a Perkin-Elmer model Spectrum One B spectrophotometer with sealed solution cell [0.1 mm (CaF_2)] windows. UV−vis spectra were recorded on an Agilent 8453 UV−vis spectroscopy system. ^{1}H NMR spectra were obtained on Varian Unity 400 and 500 spectrometers. Analyses of carbon, hydrogen, and nitrogen were obtained with a CHN analyzer (Heraeus).

Preparation of $[(NO)_2Fe(\mu\text{-}CO)(\mu\text{-}S(CH_2)_2NH_3)Fe(NO)_2]$ (1). $Fe(CO)_2(NO)_2$ (0.017 g, 0.1 mmol) and cysteamine (0.0039 g, 0.05 mmol) were dissolved in THF (20 mL) under a N_2 atmosphere at 0 °C. The reaction solution was stirred under a N_2 atmosphere for 3 h at 0 °C. The resulting solution was monitored by FTIR. The IR ν_{NO}/ν_{CO} spectra of the reaction solution showing stretching frequencies at 1693 s, 1707 s (ν_{NO}), 1851 m (ν_{CO}) cm^{-1} (THF) imply the formation of complex **1**. The dark-aquamarine solution was dried under vacuum and redissolved in THF. The dark-aquamarine solution was filtered through Celite, and hexane was then added to the filtrate to precipitate the dark-aquamarine oily complex **1**. A total of 1 equiv of 18-crown-6-ether was added to the THF solution of complex **1** for crystallization, and crystals suitable for single-crystal XRD analysis were obtained from the THF solution of complex **1** layered with hexane at −20 °C for 2 weeks (yield 0.047 g, 78%). IR: 1693 s, 1707 s (ν_{NO}), 1851 m (ν_{CO}) cm^{-1} (THF). ^{1}H NMR (C_4D_8O): δ 2.47 (s, 1H (−SH)), 2.60 (t, 2H ($-CH_2$)), 3.09 (t, 2H ($-CH_2$)), 7.31 (s, 3H ($-NH_3$)). Absorption spectrum (THF) [λ_{max}, nm (ε, M^{-1} cm^{-1})]: 384 (7880), 605 (2730). Anal. Calcd for $C_{15}H_{31}Fe_2N_5O_{11}S$: C, 29.97; H, 5.20; N, 11.65. Found: C, 30.19; H, 5.16; N, 11.35.

Preparation of $[(NO)_2Fe(\mu\text{-}S(CH_2)_2NH_2)(\mu\text{-}S(CH_2)_2NH_3)Fe(NO)_2]$ (2). To a flask containing cysteamine (0.0077 g, 0.1 mmol) and O_2 (1.23 mL, 0.05 mmol) was added the THF (20 mL) solution of complex **1** (0.060 g, 0.1 mmol). The reaction solution was stirred under a N_2 atmosphere for 48 h at ambient temperature. The resulting dark-green solution was monitored by FTIR. The IR ν_{NO}/ν_{CO} stretching frequencies shifting from 1693 s, 1707 s (ν_{NO}), 1851 m (ν_{CO}) cm^{-1} to 1658 s, 1678 s (ν_{NO}) cm^{-1} (THF) were assigned to formation of the neutral $\{Fe(NO)_2\}^{10}\{Fe(NO)_2\}^9$ rRRE **2**. The reaction solution was dried under vacuum and redissolved in THF. The dark-green THF solution was filtered through Celite, and hexane was then added to the filtrate to precipitate the dark-green solid complex **2**. Formation of the byproduct water is supported by isotopic labeling experiments. The reaction of the THF solution of complex **1**, D-cysteamine $[DS(CH_2)_2NH_2]$, and O_2 in a 1:1:0.5 molar ratio yields the byproduct DHO identified by ^{2}H NMR [δ 2.57 (THF); SI Figure S4]. Deuterated cysteamine was prepared based on the following procedure: NaH [3 mg, 0.125 mmol (80%)] added to a solution of cysteamine (7.7 mg, 0.1 mmol) in THF (10 mL) was stirred under N_2(g) at ambient temperature for 2 h. Then deuterated acetic acid (5.77 μL, 0.1 mmol) was injected into the mixture solution by syringe, and the resulting solution was stirred for 1 h. The mixture solution was concentrated to 3 mL, and then Et_2O (10 mL) was added to the mixture solution to precipitate D-cysteamine white powder and $[Na][CH_3COO]$. The white powder was redissolved in THF (3 mL). The THF solution was filtered through Celite to remove the insoluble solid $[Na][CH_3COO]$, and then the filtrate was dried under vacuum to yield the white deuterated cysteamine [yield 3.75 mg (48%)]. A total of 1 equiv of 18-crown-6-ether was added to the THF solution of complex **2** for crystallization, and crystals suitable for single-crystal XRD were obtained from the THF solution of complex **2** layered with hexane at −20 °C for 2 weeks (yield 0.045 g, 69%). IR: 1658 s, 1678 s (ν_{NO}) cm^{-1} (THF). Absorption spectrum (THF) [λ_{max}, nm (ε, M^{-1} cm^{-1})]: 320 (4610), 358 (4450), 452 (2000), 650 (1110), 962 (1380). Anal. Calcd for $C_{16}H_{37}Fe_2N_6O_{10}S_2$: C, 29.60; H, 5.74; N, 12.94. Found: C, 29.62; H, 5.73; N, 12.70.

Reaction of Complex 2 and O_2. Complex **2** (0.0649 g, 0.1 mmol) was dissolved in THF (20 mL), and then dry O_2 (1.23 mL, 0.05 mmol) was injected into a Schlenk flask by a microsyringe. The reaction solution was stirred under a N_2 atmosphere at ambient temperature for 10 min. The solution was monitored by FTIR. The IR ν_{NO} stretching frequencies shifting from 1658 s, 1678 s cm^{-1} to 1749 s, 1774 s, 1808 vw (ν_{NO}) cm^{-1} were assigned to the formation of $[(NO)_2Fe(\mu\text{-}S(CH_2)_2NH_2)]_2$ (**3**).[14,15] The reaction solution was concentrated to 5 mL, and then diethyl ether (15 mL) was added to the reaction solution. The red-brown solution was filtered through Celite to remove the insoluble solid, and then the filtrate was dried under vacuum. The red-brown oily product was redissolved in THF (2 mL) under a N_2 atmosphere, and hexane (20 mL) was added to the THF solution to precipitate the red-brown oily complex **3** (yield 0.021 g, 54%). IR: 1749 s, 1774 s, 1808 vw (ν_{NO}) cm^{-1} (THF); 1756 s, 1782 s, 1814 vw (ν_{NO}) cm^{-1} (D_2O). ^{1}H NMR (C_4D_8O): δ 1.12 (br), 1.77 (br), 3.38 (br) ($-CH_2CH_2NH_2$). Absorption spectrum (THF) [λ_{max}, nm (ε, M^{-1} cm^{-1})]: 307 (19070), 358 (11880). ESI-MS (m/z): 384.9 ($[M + H]^+$).

Preparation of $[(S(CH_2)_2NH_2)(S(CH_2)_2NH_3)Fe(NO)_2]$ (4). To a flask containing cysteamine (0.0158 g, 0.205 mmol) was added the THF (20 mL) solution of complex **3** (0.0384 g, 0.1 mmol). The reaction solution was stirred under a N_2 atmosphere for 2 h at ambient temperature. The resulting yellow-green solution was monitored by FTIR. The IR ν_{NO} stretching frequencies shifting from 1749 s, 1774 s, 1808 vw (ν_{NO}) cm^{-1} to 1685 s, 1731 s (ν_{NO}) cm^{-1} (THF) imply formation of the neutral $\{Fe(NO)_2\}^9$ DNIC **4**. Then solution was filtered through Celite, and hexane was added slowly to the filtrate to precipitate the yellow-green oily complex **4**. A total of 1 equiv of 18-crown-6-ether was added to the THF solution of complex **4** for crystallization, and crystals suitable for XRD analysis were obtained from the THF solution of complex **4** layered with hexane at −20 °C for 2 weeks (yield 0.076 g, 71%). IR: 1685 s, 1731 s (ν_{NO}) cm^{-1} (THF). Absorption spectrum (THF) [λ_{max}, nm (ε, M^{-1} cm^{-1})]: 327 (5570), 360 (2270), 435 (1010), 649 (100). Anal. Calcd for $C_{16}H_{37}FeN_4O_8S_2$: C, 36.02; H, 6.99; N, 10.50. Found: C, 36.33; H, 6.99; N, 10.49.

Preparation of the Neutral DNIC $[(SC_6H_5)(S(CH_2)_2NH_3)Fe(NO)_2]$ (5). Complex **3** (0.0384 g, 0.1 mmol) was dissolved in THF (15 mL) under nitrogen at ambient temperature. The 22 μL of thiophenol (0.205 mmol) was injected by microsyringe into the THF solution of complex **3**. After the reaction solution was stirred at ambient temperature for 1 h, the resulting red-purple solution was monitored by FTIR. The IR ν_{NO} stretching frequencies shifting from 1749 s, 1774 s, 1808 vw (ν_{NO}) cm^{-1} to 1693 s, 1739 s (ν_{NO}) cm^{-1} (THF) suggested formation of the neutral $\{Fe(NO)_2\}^9$ DNIC **5**.[21] The solution was filtered through Celite, and hexane was added slowly to the filtrate to precipitate the red-purple oily complex **5**. A total of 1

dx.doi.org/10.1021/ic402364p | Inorg. Chem. 2013, 52, 13918−13926

equiv of 18-crown-6-ether was added to the THF solution of complex **5** for crystallization, and crystals suitable for XRD analysis were obtained from the THF solution of complex **5** layered with hexane at −20 °C for 2 weeks (yield 0.082 g, 72%). IR: 1693 s, 1739 s (ν_{NO}) cm^{-1} (THF). Absorption spectrum (THF) [λ_{max}, nm (ε, M^{-1} cm^{-1})]: 322 (7110), 367 (4480), 455 (2160), 795 (290). Anal. Calcd for $C_{20}H_{36}FeN_3O_8S_2$: C, 42.40; H, 6.41; N, 7.42. Found: C, 42.19; H, 6.36; N, 6.92.

Reaction of Complex 2 and Diphenyl Disulfide. THF (15 mL) was added to a Schlenk flask containing complex **2** (0.0649 g, 0.1 mmol) and 0.0109 g of diphenyl disulfide (0.05 mmol) under nitrogen at ambient temperature. After the mixture solution was stirred for 24 h, the resulting red-purple solution was monitored by FTIR. The IR ν_{NO} stretching frequencies 1749 s, 1774 s, 1808 vw, 1693 s, 1739 s cm^{-1} suggested formation of the neutral RRE **3** and DNIC **5**. Diethyl ether was then added to the mixture solution to separate the THF−diethyl ether-soluble RRE **3** and, concomitantly, precipitate DNIC **5**. Complexes **3** and **5** were characterized by IR and UV−vis spectra.[14,15]

Preparation of $[(SC_2H_3(CO_2)(NH_3))(S(CH_2)_2NH_3)Fe(NO)_2]$ (6). MeOH (15 mL) was added to a Schlenk flask containing complex **3** (0.0384 g, 0.1 mmol) and 0.025 g of cysteine (0.205 mmol) under nitrogen at ambient temperature. After the mixture solution was stirred for 3 h, the resulting olive solution was monitored by FTIR. The IR ν_{NO} stretching frequencies shifting from 1749 s, 1774 s, 1808 vw (ν_{NO}) cm^{-1} to 1710 m, 1754 s (ν_{NO}) cm^{-1} (MeOH) suggested formation of the neutral DNIC **6**. The mixture solution was filtered through Celite, and diethyl ether was then added slowly to the filtrate to precipitate the olive solid complex **6**. A total of 1 equiv of 18-crown-6-ether was added to the THF solution of complex **6** for stabilization (yield 0.068 g, 76%). IR: 1710 m, 1754 s (ν_{NO}) cm^{-1} (MeOH); 1719 s, 1770 s (ν_{NO}) cm^{-1} (D_2O). EPR: a well-resolved 13-line hyperfine splitting EPR spectra g value of 2.03 with coupling constants $A_{N(NO)}$ = 2.36 G, $A_{H(Cys)}$ = 1.15 G. and $A_{H(cysteamine)}$ = 1.45 G) (H_2O) at 298 K. Absorption spectrum (H_2O) [λ_{max}, nm (ε, M^{-1} cm^{-1})]: 378 (5240). Anal. Calcd for $C_5H_{13}FeN_4O_4S_2 \cdot 1/2(C_{12}O_6H_{24})$: C, 29.67; H, 5.66; N, 12.58. Found: C, 29.55; H, 5.66; N, 12.09.

Preparation of the Neutral Mixed-Thiolate rRRE $[(NO)_2Fe(\mu\text{-}SC_6H_5)(\mu\text{-}S(CH_2)_2NH_3)Fe(NO)_2]$ (7). Complex **5** (0.0556 g, 0.1 mmol) was dissolved in THF (20 mL) under nitrogen at ambient temperature. $[Fe(CO)_2(NO)_2]$ (13 μL, 0.105 mmol) was added to the THF solution of complex **5** via a microsyringe under a positive pressure of N_2. After the reaction solution was stirred at ambient temperature for 2 h, the resulting dark-green solution was monitored by FTIR. The IR ν_{NO} stretching frequencies 1665 s, 1685 s (ν_{NO}) cm^{-1} (THF) were assigned to formation of the mixed-thiolate-containing rRRE **7**. The dark-green solution was filtered through Celite, and hexane was added slowly to the filtrate to precipitate the dark-green solid complex **7**. A total of 1 equiv of 18-crown-6-ether was added to the THF solution of complex **7** for stabilization (yield 0.042 g, 62%). IR: 1665 s, 1685 s (ν_{NO}) cm^{-1} (THF). EPR: an isotropic EPR signal at 1.999 (THF, 298 K) and a rhombic EPR signal at g_1 = 2.010, g_2 = 1.999, and g_3 = 1.972 (THF, 77 K). Absorption spectrum (THF) [λ_{max}, nm (ε, M^{-1} cm^{-1})]: 369 (5220), 445 (2700), 650 (845), 973 (1060). Anal. Calcd for $C_{20}H_{36}Fe_2N_5O_{10}S_2$: C, 35.20; H, 5.32; N, 10.26. Found: C, 35.08; H, 4.94; N, 9.83.

EPR Spectroscopy. EPR measurements were performed at X band using a Bruker ELEXSYS E580 spectrometer equipped with a ELEXSYS superhigh-sensitivity probehead cavity. At 77 and 298 K, X-band EPR spectra of complex **2** (THF) were obtained with frequencies at 9.660 and 9.661 GHz, respectively. The microwave power and modulation amplitude of complex **2** were 15 mW and 0.8 G at 100.00 kHz. At 77 and 298 K, X-band EPR spectra of complex **4** (MeOH) were obtained with frequencies at 9.684 and 9.686 GHz, respectively. The microwave power and modulation amplitude were 15 mW and 0.8 G at 100.00 kHz, respectively. At 77 K, X-band EPR spectra of complex **5** (THF) were obtained with a frequency at 9.658 GHz. The microwave power and modulation amplitude were 15 mW and 0.8 G at 100.00 kHz. At 298 K, X-band EPR spectra of complex **5** (THF) were obtained with a frequency at 9.657 GHz. The microwave power and modulation amplitude were 9.464 mW and 0.8 G at 100.00 kHz. At 77 and 298 K, X-band EPR spectra of complex **6** (H_2O) were obtained with frequencies at 9.662 and 9.815 GHz, respectively. The microwave power and modulation amplitude of complex **6** were 15 mW and 0.8 G at 100.00 kHz. At 77 and 298 K, X-band EPR spectra of complex **7** (THF) were obtained with frequencies at 9.658 and 9.657 GHz, respectively. The microwave power and modulation amplitude of complex **7** were 15 mW and 0.8 G at 100.00 kHz.

Magnetic Measurements. The magnetic data were recorded on a SQUID magnetometer (SQUID-VSM Quantum Design Company) under a 1 T external magnetic field for complex **2** in the temperature range 4−300 K. The magnetic susceptibility data were corrected with temperature-independent paramagnetism (2×10^{-4} cm^3 mol^{-1}), and the ligands' diamagnetism was corrected by the tabulated Pascal's constants.[22]

XAS Measurements. All Fe K-edge spectra were carried out at National Synchrotron Radiation Research Center of Taiwan (NSRRC), Hsinchu, Taiwan, and were recorded at room temperature. Experiments were performed in transmission mode at the BL17C wiggler beamline with a double-crystal Si(111) monochromator. The energy resolution $\Delta E/E$ was estimated to be about 2×10^{-4}. High harmonics were rejected by rhodium-coated mirrors. The spectra were scanned from 6.912 to 8.006 keV. A reference iron foil was always measured simultaneously, in which the first inflection point at 7112.0 eV of the iron foil spectrum was used for energy calibration. Ion chambers used to measure the incident (I_0) and transmitted (I) beam intensities were filled with a mixture of N_2 and He gases and a mixture of N_2 and Ar gases, respectively. The spectra were normalized based on the procedures reported by Solomon and co-workers.[23] A smooth background was removed from all spectra by fitting a straight line to the preedge region and then subtracting this straight line from the entire spectrum. Normalization of the data was accomplished by fitting a flat polynomial to the postregion and by normalizing the edge jump to 1.0 at 7400 eV for Fe K-edge spectra.

X-ray Crystallography. Crystallographic data and structure refinement parameters of complexes **1**, **2**, **4**, and **5** are summarized in the Supporting Information (Table S1). The crystals of complexes **1**, **2**, **4**, and **5** chosen for XRD studies were measured in sizes of 0.30 × 0.19 × 0.04, 0.34 × 0.26 × 0.13, 0.68 × 0.45 × 0.09, and 0.28 × 0.25 × 0.06 mm^3, respectively. Each crystal was mounted on a glass fiber and quickly coated in an epoxy resin. Unit-cell parameters were obtained by least-squares refinement. Diffraction measurements were carried out on a Bruker X8 APEX II CCD diffractometer for complexes **1**, **2**, **4**, and **5** with graphite-monochromated Mo Kα radiation (λ = 0.7107 Å) between 1.89 and 25.07° for complex **1**, between 1.46 and 25.00° for complex **2**, between 1.88 and 25.03° for complex **4**, and between 1.57 and 25.12° for complex **5**. Least-squares refinement of the positional and anisotropic thermal parameters of all non-hydrogen atoms and fixed hydrogen atoms was based on F^2. A semiempirical from equivalent absorption correction was made for **1**, **2**, **4**, and **5**. The *SHELXTL* structure refinement program was employed.[24] For complex **1**, remarkable electron densities (hydrogen) located around N5 were observed. For complex **4**, remarkable electron densities located around N4 and N4′ were observed as C3−C4−N4 and C3′−C4′−N4′, respectively, and assigned to cysteamine residues. This implies that the same site in two unit cells is occupied by different forms of cysteamine. The partition ratio 65:35 is used to model substitutional disorder.

■ ASSOCIATED CONTENT

Ⓢ Supporting Information

X-ray crystallographic files in CIF format for structure determinations of **1**, **2**, **4**, and **5** and NMR and FTIR spectra. This material is available free of charge via the Internet at http://pubs.acs.org.

■ AUTHOR INFORMATION

Corresponding Author

*E-mail: wfliaw@mx.nthu.edu.tw.

Notes

The authors declare no competing financial interest.

■ ACKNOWLEDGMENTS

We gratefully acknowledge financial support from the National Science Council of Taiwan. The authors thank Dr. Tsai-Te Lu for valuable discussion, Ting-Shen Kuo for single-crystal X-ray structure determinations, and Dr. M.-H. Chiang for magnetic susceptibility measurements. We also thank Dr. Jyh-Fu Lee and the NSRRC for their support of the hardware and software applied in this work.

■ REFERENCES

(1) (a) Ignarro, L. J.; Buga, G. M.; Wood, K. S.; Byrns, R. E.; Chaudhri, G.. *Proc. Natl. Acad. Sci. U.S.A.* **1987**, *84*, 9265−9269. (b) Palmer, R. M. J.; Ferrige, A. G.; Moncada, S. *Nature* **1987**, *327*, 524−526. (c) Garthwaite, J. *Eur. J. Neurosci.* **2008**, *27*, 2783−2802. (d) Bredt, D. S.; Hwang, P. M.; Snyder, S. H. *Nature* **1990**, *347*, 768−770.

(2) (a) Marietta, M. A.; Yoon, P. S.; Iyengar, R.; Leaf, C. D.; Wishnokll, J. S. *Biochemistry* **1988**, *27*, 8706−8711. (b) Bogdan, C. *Nat. Immunol.* **2001**, *2*, 907−916. (c) Jenkins, D. C.; Charles, I. G.; Thomsen, L. L.; Moss, D. W.; Holmes, L. S.; Baylis, S. A.; Rhodes, P.; Westmore, K.; Emson, P. C.; Moncada, S. *Proc. Natl. Acad. Sci. U.S.A.* **1995**, *92*, 4392−4396. (d) Reynolds, M. M.; Witzeling, S. D.; Damodaran, V. B.; Medeiros, T. N.; Knodle, R. D.; Edwards, M. A.; Lookian, P. P.; Brown, M. A. *Biochem. Biophys. Res. Commun.* **2013**, *431*, 647−651. (e) Burke, A. J.; Sullivan, F. J.; Giles, F. J.; Glynn, S. A. *Carcinogenesis* **2013**, *34*, 503−512.

(3) (a) Harrop, T. C.; Tonzetich, Z. J.; Reisner, E.; Lippard, S. J. *J. Am. Chem. Soc.* **2008**, *130*, 15602−15610. (b) Foster, M. W.; Cowan, J. A. *J. Am. Chem. Soc.* **1999**, *121*, 4093−4100. (c) Crack, J. C.; Stapleton, M. R.; Green, J.; Thomson, A. J.; Le Brun, N. E. *J. Biol. Chem.* **2013**, *288*, 11492−11502.

(4) (a) Vanin, A. F. *Nitric Oxide* **2009**, *21*, 1−13. (b) Boese, M.; Mordvintcev, P. I.; Vanin, A. F.; Busse, R.; Mulsch, A. *J. Biol. Chem.* **1995**, *270*, 29244−29249. (c) Lewandowska, H.; Kalinowska, M.; Brzoska, K.; Wojciuk, K.; Wojciuk, G.; Kruszewski, M. *Dalton Trans.* **2011**, *40*, 8273−8289.

(5) Toledo, J. C., Jr.; Bosworth, C. A.; Hennon, S. W.; Mahtani, H. A.; Bergonia, H. A.; Lancaster, J. R., Jr. *J. Biol. Chem.* **2008**, *283*, 28926−28933.

(6) (a) Suryo Rahmanto, Y.; Kalinowski, D. S.; Lane, D. J.; Lok, H. C.; Richardson, V.; Richardson, D. R. *J. Biol. Chem.* **2012**, *287*, 6960−6968. (b) Ueno, T.; Suzuki, Y.; Fujii, S.; Vanin, A. F.; Yoshimura, T. *Biochem. Pharmacol.* **2002**, *63*, 485−493.

(7) (a) Enemark, J. H.; Feltham, R. D. *Coord. Chem. Rev.* **1974**, *13*, 339−406. (b) Chiang, C. Y.; Darensbourg, M. Y. *J. Biol. Inorg. Chem.* **2006**, *11*, 359−370. (c) Hess, J. L.; Hsieh, C.-H.; Reibenspies, J. H.; Darensbourg, M. Y. *Inorg. Chem.* **2011**, *50*, 8541−8552. (d) Shih, W.-C.; Lu, T.-T.; Yang, L.-B.; Tsai, F.-T.; Chiang, M.-H.; Lee, J.-F.; Chiang, Y.-W.; Liaw, W.-F. *J. Inorg. Biochem.* **2012**, *113*, 83−93.

(8) (a) Tinberg, C. E.; Tonzetich, Z. J.; Wang, H.; Do, L. H.; Yoda, Y.; Cramer, S. P.; Lippard, S. J. *J. Am. Chem. Soc.* **2010**, *132*, 18168−18176. (b) Crack, J. C.; Smith, L. J.; Stapleton, M. R.; Peck, J.; Watmough, N. J.; Buttner, M. J.; Buxton, R. S.; Green, J.; Oganesyan, V. S.; Thomson, A. J.; Le Brun, N. E. *J. Am. Chem. Soc.* **2011**, *133*, 1112−1121.

(9) (a) Wecksler, S. R.; Hutchinson, J.; Ford, P. C. *Inorg. Chem.* **2006**, *45*, 1192−1200. (b) Wecksler, S. R.; Mikhailovsky, A.; Korystov, D.; Buller, F.; Kannan, R.; Tan, L.-S.; Ford, P. C. *Inorg. Chem.* **2007**, *46*, 395−402. (c) Fitzpatrick, J.; Kalyvas, H.; Shearer, J.; Kim, E. *Chem. Commun.* **2013**, *49*, 5550−5552. (d) Hung, M.-C.; Tsai, M.-C.; Lee, G.-H.; Liaw, W.-F. *Inorg. Chem.* **2006**, *45*, 6041−6047.

(10) Rudneva, T. N.; Sanina, N. A.; Lyssenko, K. A.; Aldoshin, S. M.; Antipin, M. Y.; Ovanesyan, N. S. *Mendeleev Commun.* **2009**, *19*, 253−255.

(11) Vanin, A. F.; Mokh, V. P.; Serezhenkov, V. A.; Chazov, E. I. *Nitric Oxide* **2007**, *16*, 322−330.

(12) (a) Wang, R.; Camacho-Fernandez, M. A.; Xu, W.; Zhang, J.; Li, L. *Dalton Trans.* **2009**, *5*, 777−786. (b) Hayter, R. G.; Williams, L. F. *Inorg. Chem.* **1964**, *3*, 717−719. (c) Chen, Y.-J.; Ku, W.-C.; Feng, L.-T.; Tsai, M.-L.; Hsieh, C.-H.; Hsu, W.-H.; Liaw, W.-F.; Hung, C.-H.; Chen, Y.-J. *J. Am. Chem. Soc.* **2008**, *130*, 10929−10938.

(13) (a) Chen, C.-H.; Chiou, S.-J.; Chen, H.-Y. *Inorg. Chem.* **2010**, *49*, 2023−2025. (b) Ueyama, N.; Nishikawa, M.; Yamada, Y.; Okamura, T.; Nakamura, A. *J. Am. Chem. Soc.* **1996**, *118*, 12826−12827.

(14) (a) Yeh, S.-W.; Lin, C.-W.; Li, Y.-W.; Hsu, I.-J.; Chen, C.-H.; Jang, L.-Y.; Lee, J.-F.; Liaw, W.-F. *Inorg. Chem.* **2012**, *51*, 4076−4087. (b) Tsou, C.-C.; Lu, T.-T.; Liaw, W.-F. *J. Am. Chem. Soc.* **2007**, *129*, 12626−12627. (c) Lu, T.-T.; Tsou, C.-C.; Huang, H.-W.; Hsu, I.-J.; Chen, J.-M.; Kuo, T.-S.; Wang, Y.; Liaw, W.-F. *Inorg. Chem.* **2008**, *47*, 6040−6050.

(15) (a) Harrop, T. C.; Song, D.; Lippard, S. J. *J. Am. Chem. Soc.* **2006**, *128*, 3528−3529. (b) Harrop, T. C.; Song, D.; Lippard, S. J. *J. Inorg. Biochem.* **2007**, *101*, 1730−1738. (c) Dillinger, S. A. T.; Schmalle, H. W.; Fox, T.; Berke, H. *Dalton Trans.* **2007**, *32*, 3562−3571. (d) Costanzo, S.; Ménage, S.; Purrello, R.; Bonomo, R. P.; Fontecave, M. *Inorg. Chim. Acta* **2001**, *318*, 1−7.

(16) Tsou, C.-C.; Tsai, F.-T.; Chen, H.-Y.; Hsu, I.-J.; Liaw, W.-F. *Inorg. Chem.* **2013**, *52*, 1631−1639.

(17) Lin, Z.-S.; Lo, F.-C.; Li, C.-H.; Chen, C.-H.; Huang, W.-N.; Hsu, I.-J.; Lee, J.-F.; Horng, J.-C.; Liaw, W.-F. *Inorg. Chem.* **2011**, *50*, 10417−10431. (b) Huang, H.-W.; Tsou, C.-C.; Kuo, T.-S.; Liaw, W.-F. *Inorg. Chem.* **2008**, *47*, 2196−2204.

(18) McDonald, C.-C.; Phillips, W. D.; Mower, H. F. *J. Am. Chem. Soc.* **1965**, *87*, 3319−3326.

(19) Tsai, M.-C.; Tsai, F.-T.; Lu, T.-T.; Tsai, M.-L.; Wei, Y.-C.; Hsu, I.-J.; Lee, J.-F.; Liaw, W.-F. *Inorg. Chem.* **2009**, *48*, 9579−9591.

(20) (a) Klein, A.; Mering, Y. V.; Uthe, A.; Butsch, K.; Schaniel, D.; Mockus, N.; Woike, T. *Polyhedron* **2010**, *29*, 2553−2559. (b) Hedberg, L.; Hedberg, K.; Satija, S. K.; Swanson, B. I. *Inorg. Chem.* **1985**, *24*, 2766−2771.

(21) Tsai, M.-L.; Liaw, W.-F. *Inorg. Chem.* **2006**, *45*, 6583−6585.

(22) (a) Bain, G. A.; Berry, J. F. *J. Chem. Educ.* **2008**, *85*, 532−536. (b) Kahn, O. *Molecular Magnetism*; VCH: New York, 1993.

(23) Solomon, E. I.; Hedman, B.; Hodgson, K. O.; Dey, A.; Szilagyi, R. K. *Coord. Chem. Rev.* **2005**, *249*, 97−129.

(24) Sheldrick, G. M. *SHELXTL, A Program for Crystal Structure Determination*; Siemens Analytical X-ray Instruments, Inc.: Madison, WI, 1994.